JPET Fast Forward. Published on October 24, 2007 as DOI: 10.1124/jpet.107.130062

JPET #130062

Title Page

[^{3}H]A-585539, A NOVEL HIGH AFFINITY α7 NEURONAL NICOTINIC RECEPTOR AGONIST: RADIOLIGAND BINDING CHARACTERIZATION TO RAT AND HUMAN BRAIN

DAVID J. ANDERSON, WILLIAM BUNNELLE, BRUCE SURBER, JIA DU, CAROL SUROWY, ELIANE TRIBOLLET, ANOUK MARGUERAT, DANIEL BERTRAND AND MURALI GOPALAKRISHNAN

Neuroscience Research, Global Pharmaceutical Research & Development, Abbott Laboratories, Abbott Park, IL (D.J.A, W.B., B.S., J.D., C.S., M.G.), and Department of Neuroscience, CMU, Geneva, Switzerland (E.T., A.M., D.B.)

JPET Fast Forward. Published on October 24, 2007 as DOI: 10.1124/jpet.107.130062
This article has not been copyedited and formatted. The final version may differ from this version.

JPET #130062

Running Title Page

Running Title: [^{3}H]A-585539 Binding to α7 nAChRs

Corresponding Author:
David J. Anderson
R-47W, AP9A
Abbott Laboratories
Abbott Park, IL 60064-6125
Phone: 847-937-5830
Fax: 847-937-9195
Email: david.j.anderson@abbott.com

Text pages: 19
Tables: 2
Figures: 7
References: 35
Abstract words: 250
Introduction words: 730
Discussion words: 1554

ABBREVIATIONS: nAChR, nicotinic acetylcholine receptor; α-Bgt, α-Bungarotoxin; MLA, methyllycaconitine; A-585539, (1S,4S)-2,2-dimethyl-5-(6-phenylpyridazin-3-yl)-5-aza-2-azoniabicyclo[2.2.1]heptane; PNU-282987, *N*-[(3*R*)-1-azabicyclo[2.2.2]oct-3-yl]-4-chlorobenzamide hydrochloride; PHA-543613, N-[(3R)-1-Azabicyclo[2.2.2]oct-3-yl]furo[2,3-c]pyridine-5-carboxamide; (±)-AR-R17779, (±)-spiro[1-azabicyclo[2.2.2]octane-3,5'-oxazolidin-2'-one]; A-582941, 2-Methyl-5-(6-phenyl-pyridazin-3-yl)-octahydro-pyrrolo[3,4-c]pyrrole; SSR-180711A, ; BSS, balanced salt solution; BSA, bovine serum albumen; PBS, phosphate buffered saline; PEI, polyethylenimine; A-85380, 3-(2(S)-azetidinylmethoxy)pyridine; PNU-120596, 1-(5-chloro-2,4-dimethoxy-phenyl)-3-(5-methyl-isoxazol-3-yl)-urea; MDL 72222, 3-tropanyl-3,5-

dichlorobenzoate; TC-5280, 2(R)-(3-Pyridyl)-1-azabicyclo[3.2.2]nonane; DMPP, 1,1-dimethyl-4-phenylpiperazinium; varenicline, 7,8,9,10-tetrahydro-6,10-methano-6*H*-pyrazino(2,3-h)(3)benzazepine.

Section Assignment: Neuropharmacology

Abstract

Receptor binding was characterized for [^{3}H]-(1S,4S)-2,2-dimethyl-5-(6-phenylpyridazin-3-yl)-5-aza-2-azoniabicyclo[2.2.1]heptane ([^{3}H]A-585539), a selective, high affinity α7 nicotinic acetylcholine receptor (nAChR) agonist with rapid kinetics, low nonspecific binding and high specific activity. At 4ºC, the association was monophasic and rapid ($t_{½}$ = 8.0 min); dissociation was slower ($t_{½}$ = 64.2 min). The K_d in rat brain at 4ºC was 0.063 nM, whereas at 22° and 37°C, the K_d values were 0.188 and 0.95 nM, respectively. In contrast, the B_{max} (34 fmol/mg protein) was unaffected by temperature. In human cortex, [^{3}H]A-585539 bound with a K_d of 0.066 nM and a B_{max} of 5.8 fmol/mg protein at 4ºC, whereas under similar conditions, specific [^{3}H]methyllycaconitine ([^{3}H]MLA) binding was not measurable. A number of agonist and antagonist nAChR ligands displaced binding to rat brain membranes with rank order of affinity similar to that for [^{3}H]MLA, and in general, a 5-10-fold higher affinity was observed for [^{3}H]A-585539 binding. There was also a good correlation of K_i values between [^{3}H]A-585539 binding to rat brain and human cortex. Use of a α7/5HT$_3$ chimera revealed that the N-terminal domain of α7 nAChR is sufficient to faithfully reproduce the pharmacology of [^{3}H]A-585539 binding. Autoradiographic studies comparing [^{3}H]A-585539 and [^{125}I]α-bungarotoxin revealed a similar pattern of labeling in the rat. In summary, [^{3}H]A-585539 was shown to have excellent binding characteristics in rat and human brain, and represents the first high affinity α7 agonist radioligand with utility in the characterization of this important nAChR subtype that is targeted towards ameliorating cognitive deficits underlying neuropsychiatric and neurodegenerative disorders.

JPET Fast Forward. Published on October 24, 2007 as DOI: 10.1124/jpet.107.130062
This article has not been copyedited and formatted. The final version may differ from this version.

Introduction

The α7 nicotinic acetylcholine receptor (nAChR) is a pentameric, rapidly activating and desensitizing ligand-gated ion channel expressed in the mammalian central nervous system. The α7 subunit is widely expressed in the brain especially in regions associated with cognitive processing, autonomic ganglia, adrenal chromaffin cells and in non-neuronal cell types. The α7 subtype is distinguished from other nAChRs by its relatively high permeability to Ca^{2+}, rapid desensitization and sensitivity to antagonists such as α-bungarotoxin (α-Bgt) and methyllycaconitine (MLA) (Ward, et al., 1990). Unlike other nAChR subtypes, the functional significance of the α7 nAChR is not only attributable to its electrogenic properties (i.e. modulation of neuronal excitability and neurotransmitter release) but also to its high Ca^{2+}-permeability and association with biochemical signaling pathways (reviewed in Role and Berg, 1996; Berg and Conroy, 2002; Dajas-Bailador and Wonnacott, 2004). At the cellular level, activation of α7 nAChRs can regulate interneuron excitability, modulate the release of excitatory and inhibitory neurotransmitters, and contribute to neuroprotective effects (for review see, Dani and Bertrand, 2007).

Recent studies with antisense, gene knockout and subtype selective ligands have provided evidence that targeting the α7 nAChRs can lead to improvements in cognitive performance and sensory gating deficits in vivo. For example, α7 nAChR genetic knockout mice have shown impaired performance in ethanol-induced contextual fear conditioning (Wehner, et al., 2004) and showed further deterioration in hippocampus-selective associative learning and memory when crossed with Tg2576 animals (Dineley, et al., 2002). Selective α7 nAChR agonists such as PNU-282987 (Hajos, et al., 2005; Bodnar et al., 2005), PHA-543613 (Wishka, et al., 2006), AR-R17779 (Van Kampen, et

JPET Fast Forward. Published on October 24, 2007 as DOI: 10.1124/jpet.107.130062
This article has not been copyedited and formatted. The final version may differ from this version.

al., 2004; Levin et al., 1999), SSR180711 (Biton, et al., 2007) and A-582941 (Bitner et al., 2007) improve performance in models thought to capture sensory gating deficit, short-term working memory and memory consolidation domains of cognitive function. Moreover, sensory gating and cognitive performance is known to be impaired in rodents with decreased expression or following pharmacological blockade of α7 nAChRs (Luntz-Leybman et al., 1992; Stevens et al., 1998; Felix and Levin, 1997; Levin and Rezvani, 2002). Consistent with this, expression of the α7 protein is reduced in the brains of patients with Alzheimer's disease (Burghaus et al., 2000) and schizophrenia (Freedman et al., 1995). The latter phenomenon has been correlated with polymorphisms in the promoter region of the α7 gene in schizophrenic patients where such polymorphisms have been shown to result in decreased gene transcription (Freedman et al., 1997; Leonard et al., 2002). These and other observations have attracted considerable attention to the α7 nAChR as a drug target in recent years, the hypothesis being that augmenting α7 nAChR function could ameliorate the cognitive deficits associated with neuropsychiatric and neurodegenerative diseases (Rezvani and Levin, 2001; Martin et al., 2004). Accordingly, selective agonists and positive allosteric modulators of α7 nAChRs are being discovered and developed for the treatment of cognitive deficits associated with neuropsychiatric and neurodegenerative disease such as schizophrenia and Alzheimer's disease.

Although the α7 nAChR continues to be explored as a target for a number of CNS indications, developments in high affinity pharmacological tools have largely been antagonists, such as the snake toxin peptide, α-bungarotoxin (α-Bgt), and the alkaloid, methyllycaconitine (MLA) and the corresponding radioligands, [^{125}I]α-bungarotoxin ([^{125}I]α-Bgt) and [^{3}H]methyllycaconitine ([^{3}H]MLA). α-Bgt has been an invaluable tool in the characterization of nAChRs in skeletal muscle, for functional studies as a pseudo-irreversible antagonist, and for labeling, purifying and

visualizing native nAChRs. Of the cloned neuronal subunits, the α7, α8 and α9 subunits are unique in that they are all sensitive to α-Bgt when expressed in *Xenopus* oocytes. MLA is a natural norditerpenoid alkaloid, identified as the principal toxic agent in *Delphinium brownie* (Ward, et al., 1990), [^{3}H]MLA binds to rat brain membranes with an affinity, pharmacological profile and regional distribution characteristic of α-Bgt-sensitive, putative α7 subunit-containing nAChRs (Davies, et al., 1999). Although [^{3}H]MLA displays rapid binding kinetics, it suffers from a relatively high degree of nonspecific binding. Unlike the heteromeric nAChRs where a number of agonist ligands (e.g. A-85380) have become available to characterize receptors in animals and humans under various drug treatment and disease conditions, high affinity α7 nAChR agonist ligands have not yet emerged.

During the course of our in-house efforts, we discovered several bicycloheptane analogs with high binding affinities towards displacement of [^{3}H]MLA. In this study, we describe (1S,4S)-2,2-dimethyl-5-(6-phenylpyridazin-3-yl)-5-aza-2-azoniabicyclo[2.2.1] heptane ([^{3}H]A-585539) as the first high affinity agonist radioligand with excellent binding characteristics across both rodent and human brain.

Methods

Synthesis of [^{3}H]A-585539: [^{3}H]Methyl iodide in toluene (250 mCi in 0.1 ml, 85 Ci/mmol, American Radiolabeled Chemicals, Inc., St Louis, MO) was combined with a solution of (1S,4S)-2-methyl-5-(6-phenylpyridazin-3-yl)-2,5-diazabicyclo[2.2.1]heptane (US Patent 20070072892(A1)) in dichloromethane (0.788 mg, 2.96 micromole in 0.45 ml). The vial was capped and the mixture was allowed to react overnight at room temperature. Methanol was added and the solvents were evaporated to yield [^{3}H]-(1S,4S)-2,2-dimethyl-5-(6-phenylpyridazin-3-yl)-5-aza-2-azoniabicyclo [2.2.1]heptane ([^{3}H]A-585539) (US Patent 20070072892(A1)) at a total activity of 42 mCi. The product was taken up in methanol for HPLC purification. The structure of [^{3}H]A-585539 along with that of [^{3}H]MLA is illustrated in Figure 1.

For purification by high performance liquid chromatography (HPLC), about 7 mCi of [^{3}H]A-585539 was evaporated to dryness and the residue was dissolved in 4.5 ml acetonitrile:water:TFA (15:85:0.1). This solution was injected (0.9 ml per run) onto a Phenomenex Luna C18(2) column (5 micron, 250 mm x 4.6 mm ID) using an Agilent HPLC system. [^{3}H]A-585539 was eluted by a gradient mobile phase from 10% B to 20% B in 20 min where Mobile Phase A = 0.1% trifluoroacetic acid in water and Mobile Phase B = 0.1% trifluoroacetic acid in acetonitrile at a flow rate of approximately 1 ml/min. Peak detection and chromatograms were obtained with an Agilent variable wavelength UV detector set at 275 nm. The fractions containing [^{3}H]A-585539 were collected at approximately 14 minutes using an Agilent fraction collector. The fractions were combined and the solvents were evaporated *in vacuo*. The residue was dissolved in absolute ethanol (2 ml) to give 0.7 mCi.

JPET Fast Forward. Published on October 24, 2007 as DOI: 10.1124/jpet.107.130062
This article has not been copyedited and formatted. The final version may differ from this version.

[^{3}H]A-585539 was assayed using an Agilent 1100 series HPLC system consisting of a quaternary pump, an autosampler, and a photodiode array UV detector. A Packard Radiomatic A 500 radioactivity detector was connected to the HPLC system. For radiodetection, a 500 µl flow cell and a 3:1 ratio of Ultima-Flo M scintillation cocktail to HPLC mobile phase were used. The analyses were performed using a Phenomenex Luna C18(2) column (5 microns, 250 mm x 4.6 mm ID). The mobile phase consisted of a gradient starting with 10% B and ramping to 20% B in 20 minutes followed by ramping to 90% B in 1 minute and hold at 90% B for 9 minutes, where Mobile Phase A = 0.1% trifluoroacetic acid in water and Mobile Phase B = 0.1% trifluoroacetic acid in acetonitrile. The flow rate was set at approximately 1 ml/min and the UV detection was set at 275 nm. The radiochemical purity of [^{3}H]A-585539 was found to be >98%. The specific activity was determined to be 62.78 Ci/mmol by mass spectroscopy.

[^{3}H]A-585539 Binding: [^{3}H]A-585539 ([^{3}H]-(S,S)-2,2-dimethyl-5-(6-phenyl-pyridazin-3-yl)-5-aza-2-azonia-bicyclo[2.2.1]heptane iodide, 62.8 Ci/mmol) binding was determined using membrane enriched fractions (Sullivan and Anderson, 1998) from rat brain (minus cerebellum) or human cortex (ABS Inc., Wilmington, DE). Pellets were thawed at 4°C, washed and resuspended with a Polytron at a setting of 7 in 30 volumes of BSS-Tris buffer (120 mM NaCl, 5 mM KCl, 2 mM $CaCl_2$, 2 mM $MgCl_2$, and 50 mM Tris-Cl, pH 7.4, 4°C). For saturation binding isotherms, sixteen concentrations of [^{3}H]A-585539 (0.01-2 nM) in quadruplicate and homogenate containing 100-200 µg of protein were incubated in a final volume of 500 µl for 90 minutes at 4°C. Non-specific binding was determined in the presence of 30 µM MLA. For concentration-inhibition assays, seven log-dilution concentrations of test compounds in duplicate, homogenate containing 100-200 µg of protein, and

JPET Fast Forward. Published on October 24, 2007 as DOI: 10.1124/jpet.107.130062
This article has not been copyedited and formatted. The final version may differ from this version.

0.5 nM [^{3}H]A-585539 were incubated in a final volume of 500 µl for 60 minutes at 4°C. Non-specific binding in quadruplicate was determined in the presence of 10 µM MLA. Bound radioactivity was collected by vacuum filtration onto Millipore MultiScreen® harvest plates FB presoaked with 0.3% polyethyleneimine using a Packard cell harvester. The filters were then rapidly rinsed with 2 ml of ice-cold BSS. PerkinElmer MicroScint-20® scintillation cocktail (40 µl) was added to each well and bound radioactivity was determined using a PerkinElmer TopCount® instrument. Binding studies were also performed using HEK-293 cells expressing an α7/5HT$_3$ chimera containing ligand-binding domain of α7 nAChR and the transmembrane/pore forming region of 5-HT$_3$ receptor. Using RT-PCR, the coding sequence for the N-terminal 224 amino acids of human α7 nicotinic receptor (α7 nAChR, protein AAA83561) and that for the C-terminal 242 amino acids of human 5-hydroxytryptamine type-3 (5-HT$_3$) serotonin receptor (protein AAP35868) were amplified with overlapping ends. Recombinant PCR using these two overlapping fragments yielded the open reading frame of the chimeric receptor. HEK-293 cells were transfected and stable transfectants maintained using standard procedures. To harvest, the cells were rinsed with PBS, scraped from flasks, and centrifuged at 1000 x g. Pellets were homogenized with a Polytron at a setting of 7 for 30 sec in 30 volumes of BSS-Tris buffer and diluted to yield about 5 µg protein per well. Binding conditions were similar to those described above.

[^{3}H]Methyllycaconitine (MLA) Binding: Assay conditions were similar to those for [^{3}H]A-585539 binding. Membrane enriched fractions from rat brain were thawed, washed and resuspended in 30 volumes of BSS-Tris buffer (120 mM NaCl, 5 mM KCl, 2 mM $CaCl_2$, 2 mM $MgCl_2$, and 50 mM Tris-Cl, pH 7.4, 22°C). Samples containing 100-200 µg of protein, 5 nM [^{3}H]MLA (25 Ci/mmol; Tocris Bioscience, Ellisville, MO) and 0.1% bovine serum albumin (BSA, Sigma, St. Louis, MO)

were incubated in a final volume of 500 µl for 60 minutes at 22°C. Seven log-dilution concentrations of each compound were tested in duplicate. Nonspecific binding was determined in the presence of 10 µM MLA. Bound radioactivity was isolated by vacuum filtration onto Millipore MultiScreen® harvest plates FB presoaked with 2% BSA. The plates were rinsed and counted as above.

Light Microscopic Autoradiography: Two 2-month-old adult rats of the Sprague-Dawley strain were killed by decapitation under pentobarbital anesthesia (50 mg/kg body weight, i.p., following ethical rules of animal rights, Geneva, Switzerland), brains dissected out and frozen by immersion in 2-methylbutane at -25°C. Serial sections (14 µm) were cut through the diencephalons in a cryostat, thaw-mounted on gelatin-chrome-alum-coated slides and stored at -80°C until use. Two series of sections were incubated with [^{3}H]A-585539 at 25 nM and 50 nM respectively. Four series of adjacent sections were incubated with [^{3}H]A-585539 at the same concentrations together with either nicotine tartrate (1 mM) or unlabeled A-585539 (500 µM). Remaining series were incubated with [^{125}I]α-bungarotoxin at 1 nM either alone or together with 300 µM of nicotine tartrate. The binding procedure was conducted as previously described (Tribollet et al., 2004). Sections incubated with [^{3}H]A-585539 were apposed for 3 weeks to a tritium-sensitive storage phosphor screen. Digital images were obtained with a phosphor imaging system (Cyclone storage Phosphor System, PerkinElmer, Shelton, CT) and Optiquant, a Windows-based software. Sections incubated with [^{125}I]α-bungarotoxin were placed in X-ray cassettes in contact with β_{max} hyperfilms (Amersham, Buckinghamshire, UK) for 3 days. Films were developed in Kodak D19 (Kodak SA, Lausanne, Switzerland) and photographed with a digital camera.

*Data Analysis***:** Dissociation constant (K_d) and maximum binding (B_{max}) values from saturation binding and observed association rate (k_{ob}) and dissociation rate (k_{off}) from kinetic experiments were determined using GraphPad Prism (Graphpad Software, San Diego, CA). The K_d was determined from the equation $K_d = k_{off}/k_{on}$, where $k_{on} = (k_{ob}-k_{off})/L$, where L is the concentration of radioligand. The IC_{50} values were determined by nonlinear regression in Microsoft® Excel or Assay Explorer. K_i values were calculated from the IC_{50} values using the Cheng-Prusoff equation, where $K_i = IC_{50}/(1+[Ligand]/K_d)$.

JPET Fast Forward. Published on October 24, 2007 as DOI: 10.1124/jpet.107.130062
This article has not been copyedited and formatted. The final version may differ from this version.

Results

Saturation Binding:

Specific binding of [^{3}H]A-585539 to rat brain membranes was saturable, rapid and represented 80-95% of total binding over the concentration range (0.01 to 2 nM) examined (Figure 2A). In saturation binding isotherms, nonlinear regression analysis of specific binding revealed an apparent dissociation constant (K_d) of 0.063 ± 0.004 nM and a maximal binding capacity (B_{max}) of 33.7 ± 1.1 fmol/mg protein (n = 8) at 4°C. Nonspecific binding was less than 10% of total binding at concentrations up to ten times the K_d. At 22°C, the K_d was 0.188 nM and the B_{max} was 31.7 fmol/mg protein (n = 5). In contrast, the binding of [^{3}H]-methyllycaconitine to rat membranes at 22°C was found to have a K_d of 1.26 ± 0.33 nM and a B_{max} of 32.7 ± 5.8 fmol/mg protein (n = 3). However, nonspecific binding of [^{3}H]MLA ranged from 20-50% of total binding even with the addition of 0.1% BSA to the incubation.

The high specific activity and excellent affinity of [^{3}H]A-585539 made it possible to directly detect binding to human brain (Figure 2B). Human frontal cortex membranes bound [^{3}H]A-585539 at 4°C with a K_d value of 0.066 ± 0.006 nM, comparable to that of rat brain, and a B_{max} of 5.8 ± 0.5 fmol/mg protein (n = 8), which is lower than observed in the rat brain. Nonspecific binding ranged from 15-50% of total binding for range of concentrations of [^{3}H]A-585539. In constrast, specific binding of [^{3}H]MLA to human frontal cortex membranes was not detectable due to low counts and high nonspecific binding levels.

Kinetics of [^{3}H]A-585539 Binding:

JPET Fast Forward. Published on October 24, 2007 as DOI: 10.1124/jpet.107.130062
This article has not been copyedited and formatted. The final version may differ from this version.

[^{3}H]A-585539 binding was temperature-dependent. Kinetic analysis demonstrated temperature-dependence for the dissociation rate, but not for the association rate (Figure 3A and B). The association half-time ($t_{1/2}$) for [^{3}H]A-585539 binding at 4°C was 8.0 ± 0.8 min and the dissociation $t_{1/2}$ was 64.2 ± 6.1 min (n = 5). Calculation of the dissociation constant from kinetic rate constants yielded a K_d of 0.021 ± 0.003 nM, which is in reasonable agreement with the K_d value obtained from saturation binding isotherms. At 22°C, the association $t_{1/2}$ (7.4 ± 0.7 min) was comparable to that obtained at 4°C, whereas the dissociation $t_{1/2}$ was much faster (7.3 ± 0.5 min, n = 4). The rapid k_{off} rate at 22°C precludes the determination of meaningful dissociation constant by typical filtration assays.

Displacement Profile of [^{3}H]A-585539:

The radioligand binding pharmacology of [^{3}H]A-585539 was assessed by examining the displacement of specific binding by agonists, antagonists and positive allosteric modulators from rat and human brain membranes (Figures 4 and 5). A number of α7-selective nAChR compounds including unlabeled A-585539, MLA, PNU-282987, (±)-AR-R17779, α-bungarotoxin, and A-582941 were found to displace [^{3}H]A-585539 and [^{3}H]MLA binding with the similar rank order of affinity. Other nAChR ligands such as (±)-epibatidine, (-)-nicotine, (-)-cytisine, (+)-anatoxin-A, varenicline, and A-85380 also exhibited a high degree of correlation (Figure 5, Table 2). In general, a shift in K_i values were observed between [^{3}H]A-585539 and [^{3}H]MLA binding displacement in rat brain membranes. Displacement of [^{3}H]A-585539 binding to human cortex membranes yielded nearly identical K_i values as for rat brain membranes (Figure 4C, Table 2). An interesting exception is MLA, which showed considerably lower apparent affinity for human cortex membranes. Positive

JPET Fast Forward. Published on October 24, 2007 as DOI: 10.1124/jpet.107.130062
This article has not been copyedited and formatted. The final version may differ from this version.

allosteric modulators of α7 nAChRs including 5-hydroxyindole and PNU-120596, neither displaced nor enhanced [^{3}H]A-585539 binding under the present experimental conditions.

To determine specificity of A-585539 for the α7 nAChR, the compound was further evaluated in a radioligand binding screen panel containing representatives of multiple G-protein coupled receptors, and ligand- and voltage-gated ion channel binding sites at CEREP (Receptor binding and Enzyme Profile; CEREP, Potiers, France). A-585539 at 10 μM did not show significant displacement of binding of over 75 targets with the exception of 5-HT$_3$ receptors where 89% inhibition of [^{3}H]-BRL 43694 (granisetron) binding was observed with 10 μM A-585539. The 5-HT$_3$ antagonist, MDL 72222, does not significantly inhibit [^{3}H]A-585539 binding to rat brain at concentrations up to 10 μM. Conversely, MDL 72222 inhibited the binding of the 5-HT$_3$ antagonist, [^{3}H]GR65630, to human 5-HT$_3$ serotonin receptors with a K_i of 12 nM while A-585539 had a K_i of 1.4 μM (*unpublished observations*).

Localization of [^{3}H]A-585539 Binding:

To assess the regions on α7 nAChRs responsible for binding interactions, studies were conducted using a α7/5HT$_3$ chimera where the N-terminal domain of α7 nAChR was fused with the transmembrane/pore-forming region of the 5-HT$_3$ receptor. [^{3}H]A-585539 showed no detectable binding to 5-HT$_3$ receptors (data not shown), whereas specific and saturable binding of [^{3}H]A-585539 was detected in cells expressing the α7/5HT$_3$ chimera (Figure 6A). Binding was rapid and represented >95% of total binding over the concentration range (0.05 to 5 nM) examined. Saturation binding isotherms revealed an apparent dissociation constant (K_d) of 0.801 ± 0.118 nM and a maximal binding capacity (B_{max}) of 10,500 ± 1000 fmol/mg protein (n = 4). The pharmacology of

JPET Fast Forward. Published on October 24, 2007 as DOI: 10.1124/jpet.107.130062
This article has not been copyedited and formatted. The final version may differ from this version.

[^{3}H]A-585539 binding was found to be consistent with an interaction with α7 nAChRs. A number of α7 nAChR-selective compounds including MLA, TC-5280, PNU-282987, α-bungarotoxin, and SSR180711A were found to displace [^{3}H]A-585539 binding with the same rank order of affinity as seen in rat brain. Non α7 nAChR-selective nAChR compounds such as (±)-epibatidine, (-)-nicotine, (+)-anatoxin-A, DMPP, varenicline and A-85380 had a high degree of correlation for displacement between α7/5HT$_3$ chimera-expressing cells and rat brain (Figure 6B). Overall, there was a coefficient of correlation of 0.94 and a slope of 1.0.

Regional Distribution of [^{3}H]A-585539 Binding:

Autoradiography studies using [^{3}H]A-585539 in rat brain showed a distribution of binding comparable to that of [^{125}I]α-bungarotoxin, with high level of binding in hippocampus and the superficial gray layer of the superior colliculus (Figure 7A). Binding was fully displaced by unlabeled A-585539 (Figure 7C). Nicotine also effectively displaced binding, although some residual labelling was seen in the CA3 area of the hippocampus (Figure 7B). In contrast, the intense labelling yielded by [^{125}I]α-bungarotoxin, in particular in the hippocampus and in the superior colliculus, (Figure 7D) was fully displaced (Figure 7E).

JPET Fast Forward. Published on October 24, 2007 as DOI: 10.1124/jpet.107.130062
This article has not been copyedited and formatted. The final version may differ from this version.

Discussion

Selective modulation of α7 nicotinic acetylcholine receptors (nAChRs) is thought to regulate cellular processes impaired in schizophrenia, Alzheimer's disease and other dementias. Our laboratory and others have previously reported on the synthesis of novel analogs derived from various diamines exemplified by SSR180711 (Biton et al., 2007) and A-582941 (Bitner et al., 2007), and quinuclidine derivatives such as PNU-282987 (Hajos et al., 2005; Bodnar et al., 2005), PHA-543613 (Wishka et al., 2006) and AR-R17779 (Van Kampen et al., 2004; Levin et al., 1999) as α7 nAChR agonists. Despite the heightened interest in this molecular target for a number of CNS indications, developments in high affinity radioligands, especially agonists with which to study this important subtype, have been less forthcoming. In the course of our discovery efforts to develop novel selective α7 nAChR agents from a series of 2.2.1 diamines, we found the diazabicyclohepane analog, A-585539, to have greater than 1000-fold selectivity for α7 nAChRs over α4β2 nAChRs in radioligand binding. Initial experiments in *Xenopus* oocytes expressing rat α7 nAChRs showed that A-585539 activated ionic currents with an EC_{50} of 0.61 μM (95% c.i. 0.29 – 1.2 μM) μM and efficacy of 94.0 ± 6.4% (n = 3). No agonist activity was detected at concentrations up to 100 μM in IMR-32 neuroblastomas or in transfected cell lines containing α3β2, α3β4, α4β2, or α4β4 nAChRs using FLIPR-based calcium flux assays (*unpublished observations*). Given that A-585539 could be modified using a tritium methylation, it was chosen as a suitable candidate for radiolabelling. Here, we describe the characterization of [^{3}H]A-585539, one of the first selective, high affinity α7 agonist radioligand with rapid kinetics, low nonspecific binding and high specific activity.

JPET Fast Forward. Published on October 24, 2007 as DOI: 10.1124/jpet.107.130062
This article has not been copyedited and formatted. The final version may differ from this version.

[^{3}H]A-585539 bound to rat brain and to human frontal cortex membranes with high affinity, and with a pharmacological profile akin to that of [^{3}H]MLA, a well-characterized α7 nAChR antagonist (Ward et al., 1990; Davies et al, 1999; Whiteaker et al, 1999). Saturation binding isotherms revealed comparable binding affinities in rat (63 pM) and human (66 pM), whereas analysis of receptor density demonstrated that human cortex expressed some 6-fold lower density of binding sites compared to the rat. A similar ratio and density was previously observed with [^{125}I]α-Bgt in rat P2 membranes (35 fmol/mg protein) and human cortex (5 fmol/mg protein) (Davies et al, 1999; Falk et al., 2003). The high affinity and high specific activity (63 Ci/mmol) of [^{3}H]A-585539 allowed for reliable pharmacological analysis of the low density of receptors in the human brain. This is a distinct advantage over [^{3}H]MLA which, with an affinity of 2 nM, does not generate measurable labeling of α7 nAChRs in human membranes under standard experimental conditions. An additional attribute of [^{3}H]A-585539 is its relatively low nonspecific binding. At concentrations near the K_d, the nonspecific binding accounts for only 5% of total binding in rat brain, and about 20% in human brain. In contrast, with [^{3}H]MLA binding, substantially higher levels of nonspecific binding (about 35% at K_d) were observed in rat brain even with the addition of 0.1% BSA in the incubation. Another limitation with [^{3}H]MLA binding is the existence of displaceable binding from glass fiber filters, which can be reduced to some extent by presoaking the filter plates with 2% BSA. Such limitations were not encountered with [^{3}H]A-585539.

The kinetics of binding of [^{3}H]A-585539 at 4ºC were rapid for association ($t_{1/2}$ = 8.0 min) and slower for dissociation ($t_{1/2}$ = 64 min) which allows for vacuum filtration assays. The K_d value determined from kinetic experiments, 21 pM, is in reasonable agreement with values obtained from equilibrium binding experiments. At 22ºC, the association rate was similar ($t_{1/2}$ = 7.4 min), although

the dissociation rate was more rapid ($t_{1/2}$ = 7.3 min) compared to that observed at 4°C. From saturation binding isotherms, the estimated K_d was 188 pM which is some 8-fold lower than the value measured at 4°C. Under similar conditions, the K_d for [^{3}H]MLA binding did not show temperature dependence (*unpublished observations*). The lower affinity of binding observed with [^{3}H]A-585539 at increased temperatures is characteristic of thermodynamic discrimination of binding kinetics in which enthalpy-driven processes produce a temperature-dependent shift in apparent affinity, unlike entropy-driven processes that do not exhibit temperature-dependent shifts in affinity (Borea et al., 1998). These observations are consistent with thermodynamic analysis with [^{3}H]cytisine binding that predominantly labels high affinity α4β2 nAChRs, where it was shown that agonist binding was both enthalpy and entropy driven, whereas antagonist binding was totally entropy driven (Borea et al., 2000).

Displacement of [^{3}H]A-585539 binding by structurally diverse nAChR ligands including agonists and antagonists indicate a rank order of selectivity characteristic of α7-selective binding (Table 2 and Fig. 4) with A-588539 showing highest affinity. In general, a good correlation between log K_i values for inhibition of [^{3}H]A-585539 binding from both rat brain and human cortex membranes was observed. A notable exception is MLA that, interestingly, had a 10-fold greater affinity for rat brain than for human cortex. This may be an additional reason why [^{3}H]MLA binding was not measurable in human cortex in our hands. When displacement of [^{3}H]A-585539 binding in rat brain membranes was compared to displacement of [^{3}H]MLA binding in the same tissue (Table 2 and Fig. 5), an excellent correlation was noted. However, compounds showed some 5-10 fold higher affinity in displacement of [^{3}H]A-585539 binding relative to [^{3}H]MLA, which may be related to the temperature-dependent shift in affinity with [^{3}H]A-585539.

JPET Fast Forward. Published on October 24, 2007 as DOI: 10.1124/jpet.107.130062
This article has not been copyedited and formatted. The final version may differ from this version.

To further investigate the regions responsible for high affinity interactions of [^{3}H]A-585539 binding, we assessed its interaction with a chimeric α7 nAChR, the α7/5HT$_3$ chimera, where the N-terminal domain of the human 5-HT$_3$ receptor is replaced with the N-terminal domain of the human α7 nAChR. Figure 6 shows [^{3}H]A-585539 binding to the α7/5HT$_3$ chimera where high levels of expression of the chimeric receptor could be detected. The log K_i values for the displacement by a range of ligands at the α7/5HT$_3$ chimera were highly correlated to the log K_i values obtained in rat brain membranes. In general, incorporation of the N-terminal domain of α7 nAChR alone is sufficient to faithfully reproduce the pharmacology of [^{3}H]A-585539 binding. Interestingly, even though the transmembrane/pore forming region of 5-HT$_3$ receptor has a similar protein structure and a relatively high degree of homology with the α7 nAChR, the K_d of 0.8 nM represents some 10-fold decrement in the affinity of [^{3}H]A-585539 binding. This relatively lower affinity is also translated across the range of nAChR compounds tested, as reflected in the leftward shift of the correlation curve when comparing log K_i values. This implies that regions beyond the N-terminal domain of the α7 nAChR may also be involved in the formation of the binding pocket responsible for high affinity binding interactions of [^{3}H]A-585539.

The conventional target for α7 nAChR drug discovery has focused on the "agonist"-binding site of nAChRs with the emergence of several agonist and competitive antagonists. More recently, ligands that are positive allosteric modulators of α7 nAChRs have been identified (Hurst et al., 2005; Gronlein et al., 2007; reviewed in Faghih et al., 2007). The positive allosteric modulators, 5-hydroxyindole and PNU-120596, failed to displace or increase [^{3}H]A-585539 or [^{3}H]MLA binding to brain membranes. This is consistent with the notion that unlike agonists, positive allosteric

modulators do not directly activate or desensitize receptors by interacting with orthosteric binding sites, but instead they enhance the sensitivity and/or efficacy of the receptor during agonist activation (Bertrand and Gopalakrishnan, 2007).

In autoradiography studies, [^{3}H]A-585539 displayed a regional binding pattern similar to that observed with [^{125}I]-α-bungarotoxin (Fig. 7). Both ligands labeled comparable regions of the rat brain with highest density of binding in the CA3 area of the hippocampus (CA3) and the superficial gray layer of the superior colliculus (SuG). While unlabelled A-585539 fully displaced [^{3}H]A-585539 binding, 1 mM nicotine did not completely displace the [^{3}H]A-585539 label in the CA3 region of the hippocampus, an area that was intensely labeled by [^{3}H]A-585539. It is possible that [^{3}H]A-585539 labeled a small population of nAChRs in this discrete area that are resistant to displacement by nicotine. However, since the concentration of [^{3}H]A-585539 used was 25 μM, which is about 400-fold above the K_d, it is also possible that small amounts of a localized non-nAChR receptor were labeled. Absolute comparison of the two radioligands is difficult because of the difference in attainable resolution between tritium and iodine-125. Phosphor imaging of tritium is inferior to film imaging of iodine-125, both in terms of visualization of structures and duration of exposure. Nonetheless, the obtained images show clearly that the highest levels of [^{3}H]A-585539 binding are observed in regions known to have high density of α7 nAChRs.

In summary, [^{3}H]A-585539 demonstrates high affinity binding consistent with α7 nAChR pharmacology, a rapid association rate and a relatively slow dissociation rate – the latter attributes, coupled with low nonspecific binding, make it ideal for filtration assays. It provides an advantage to be able to study agonist-agonist interactions at the α7 nAChR without having to interpret agonist

displacement of tenacious antagonists. [^{3}H]A-585539 binding also avoids the pitfalls of working with the pseudo-irreversible [^{125}I]α-Bgt that requires 37ºC incubation and the reversible nonspecific binding of [^{3}H]MLA. A key advantage of [^{3}H]A-585539 is that it enables the measurement of α7 nAChRs in a variety of tissues, especially human brain, unlike MLA, and should aid in the further study of ligand interactions with the α7 nAChR subtype under physiological and pathological conditions.

Acknowledgments

We thank Steven Cassar for generating the chimera construct and Kirsten Thorin-Hagene for generating the HEK-293 cell line.

References

Berg DK and Conroy WG (2002) Nicotinic alpha 7 receptors: synaptic options and downstream signaling in neurons. *J Neurobiol* 53:512-523.

Bertrand D and Gopalakrishnan M (2007) Allosteric modulation of nicotinic acetylcholine receptors. *Biochem Pharmacol* 74: 1155-1163.

Bitner RS, Bunnelle WH, Anderson DJ, Buccafusco J, Curzon P, Decker MW, Frost J M, Gronlien JH, Gubbins, E Li. J, Malysz J, Markosyn S, Marsh K, Meyer MD, Nikkel AL, Radek RJ, Robb HM, Timmermann D, Sullivan JP and Gopalakrishnan M (2007) Broad-spectrum efficacy across cognitive domains by α7 nicotinic acetylcholine receptor agonism correlates with activation of ERK1/2 and CREB phosphorylation pathways. *J Neurosci* 27(39):10578-10587.

Biton B, Bergis OE, Galli F, Nedelec A, Lochead AW, Jegham S, Godet D, Lanneau C, Santamaria R, Chesney F, Leonardon J, Granger P, Debono MW, Bohme GA, Sgard F, Besnard F, Graham D, Coste A, Oblin A, Curet O, Vige X, Voltz C, Rouquier L, Souilhac J, Santucci V, Gueudet C, Francon D, Steinberg R, Griebel G, Oury-Donat F, George P, Avenet P, Scatton B (2007) SSR180711, a novel selective alpha7 nicotinic receptor partial agonist: (1) binding and functional profile. *Neuropsychopharmacology* 32:1-16.

Bodnar AL, Cortes-Burgos LA, Cook KK, Dinh DM, Groppi VE, Hajos M, Higdon NR, Hoffmann WE, Hurst RS, Myers JK, Rogers BN, Wall TM, Wolfe ML, Wong E (2005) Discovery and structure-activity relationship of quinuclidine benzamides as agonists of alpha7 nicotinic acetylcholine receptors. *J Med Chem* 48:905-908.

Borea PA, Varani K, Gessi S, Gilli P and Gilli G (1998) Binding thermodynamics at the human neuronal nicotine receptor. *Biochem Pharmacol* 55:1189-1197.

Borea PA, Dalpiaz A, Varani K, Gilli P, Gilli G (2000) Can thermodynamic measurements of receptor binding yield information on drug affinity and efficacy? *Biochem Pharmacol* 60:1549-1556.

Burghaus L, Schutz U, Krempel U, de Vos RA, Jansen Steur EN, Wevers A, Lindstrom J and Schroder H (2000) Quantitative assessment of nicotinic acetylcholine receptor proteins in the cerebral cortex of Alzheimer patients. *Brain Res Mol Brain Res* 76:385-388.

Dajas-Bailador F and Wonnacott S (2004) Nicotinic acetylcholine receptors and the regulation of neuronal signalling. *Trends Pharmacol Sci* 25:317-324.

Dani JA and Bertrand D (2007) Nicotinic acetylcholine receptors and nicotinic cholinergic mechanisms of the central nervous system. *Annu Rev Pharmacol Toxicol* 47:699-729.

Davies AR, Hardick DJ, Blagbrough IS, Potter BV, Wolstenholme AJ and Wonnacott S (1999) Characterisation of the binding of [3H]methyllycaconitine: a new radioligand for labelling alpha 7-type neuronal nicotinic acetylcholine receptors. *Neuropharmacology* 38:679-690.

Dineley KT, Xia X, Bui D, Sweatt JD and Zheng H (2002) Accelerated plaque accumulation, associative learning deficits, and up-regulation of alpha 7 nicotinic receptor protein in transgenic mice co-expressing mutant human presenilin 1 and amyloid precursor proteins. *J Biol Chem* 277:22768-22780.

Faghih, R., Gfesser, G. and Gopalakrishnan, M. Advances in the discovery of novel positive allosteric modulators of the α7 nicotinic acetylcholine receptor. *Recent Patents on CNS Drug Discovery* 2: 99-106, 2007.

Falk L, Nordberg A, Seiger A, Kjaeldgaard A, Hellstrom-Lindahl E (2003) Higher expression of alpha7 nicotinic acetylcholine receptors in human fetal compared to adult brain. *Brain Res Dev Brain Res* 142:151-160.

Felix R and Levin ED (1997) Nicotinic antagonist administration into the ventral hippocampus and spatial working memory in rats. *Neuroscience* 81:1009-1017.

Freedman R, Hall M, Adler LE and Leonard S (1995) Evidence in postmortem brain tissue for decreased numbers of hippocampal nicotinic receptors in schizophrenia. *Biol Psychiatry* 38:22-33.

Freedman R, Coon H, Myles-Worsley M, Orr-Urtreger A, Olincy A, Davis A, Polymeropoulos M, Holik J, Hopkins J, Hoff M, Rosenthal J, Waldo MC, Reimherr F, Wender P, Yaw J, Young DA, Breese CR, Adams C, Patterson D, Adler LE, Kruglyak L, Leonard S and Byerley W (1997) Linkage of a neurophysiological deficit in schizophrenia to a chromosome 15 locus. *Proc Natl Acad Sci U S A* 94:587-592.

Gronlein J-H, Håkerud M, Ween H, Thorin-Hagene K, Briggs CA, Gopalakrishnan M and Malysz J, (2007) Distinct profiles of α7 nAChR positive allosteric modulation revealed by structurally diverse chemotypes. *Molecular Pharmacol* 72: 715-724.

Hajos M, Hurst RS, Hoffmann WE, Krause M, Wall TM, Higdon NR and Groppi VE (2005) The selective alpha7 nicotinic acetylcholine receptor agonist PNU-282987 [N-[(3R)-1-Azabicyclo[2.2.2]oct-3-yl]-4-chlorobenzamide hydrochloride] enhances GABAergic synaptic activity in brain slices and restores auditory gating deficits in anesthetized rats. *J Pharmacol Exp Ther* 312:1213-1222.

Hurst RS, Hajos M, Raggenbass M, Wall TM, Higdon NR, Lawson JA, Rutherford-Root KL, Berkenpas MB, Hoffmann WE, Piotrowski DW, Groppi VE, Allaman G, Ogier R, Bertrand

S, Bertrand D, Arneric SP (2005) A novel positive allosteric modulator of the alpha7 neuronal nicotinic acetylcholine receptor: in vitro and in vivo characterization. *J Neurosci* 25:4396-4405.

Leonard S, Gault J, Hopkins J, Logel J, Vianzon R, Short M, Drebing C, Berger R, Venn D, Sirota P, Zerbe G, Olincy A, Ross RG, Adler LE and Freedman R (2002) Association of promoter variants in the alpha7 nicotinic acetylcholine receptor subunit gene with an inhibitory deficit found in schizophrenia. *Arch Gen Psychiatry* 59:1085-1096.

Levin ED, Bettegowda C, Blosser J and Gordon J (1999) AR-R17779, and alpha7 nicotinic agonist, improves learning and memory in rats. *Behav Pharmacol* 10:675-680.

Levin ED and Rezvani AH (2002) Nicotinic treatment for cognitive dysfunction. *Curr Drug Targets CNS Neurol Disord* 1:423-431.

Luntz-Leybman V, Bickford PC and Freedman R (1992) Cholinergic gating of response to auditory stimuli in rat hippocampus. *Brain Res* 587:130-136.

Martin LF, Kem WR and Freedman R (2004) Alpha-7 nicotinic receptor agonists: potential new candidates for the treatment of schizophrenia. *Psychopharmacology (Berl)* 174:54-64.

Rezvani AH and Levin ED (2001) Cognitive effects of nicotine. *Biol Psychiatry* 49:258-267.

Role LW and Berg DK (1996) Nicotinic receptors in the development and modulation of CNS synapses. *Neuron* 16:1077-1085.

Stevens KE, Kem WR, Mahnir VM and Freedman R (1998) Selective alpha7-nicotinic agonists normalize inhibition of auditory response in DBA mice. *Psychopharmacology (Berl)* 136:320-327.

Sullivan JP and Anderson DJ (1998) Characterization of neuronal nicotinic acetylcholine receptors. In: *Current Protocols in Pharmacology* (Enna SJ, Williams M, Ferkany JW, Porsolt RD, Kenakin T and Sullivan JP, eds.) pp 1:1.8.1-1.8.9, Wiley, New York.

Tribollet E, Bertrand D, Marguerat A, and Raggenbass M (2004) Comparative distribution of nicotinic receptor subtypes during development, adulthood and aging: an autoradiographic study in the rat brain. *Neuroscience* 124:405-420.

Van Kampen M, Selbach K, Schneider R, Schiegel E, Boess F and Schreiber R (2004) AR-R 17779 improves social recognition in rats by activation of nicotinic alpha7 receptors. *Psychopharmacology (Berl)* 172:375-383.

Ward JM, Cockcroft VB, Lunt GG, Smillie FS, Wonnacott S (1990) Methyllycaconitine: a selective probe for neuronal alpha-bungarotoxin binding sites. *FEBS Lett* 270:45-48.

Wehner JM, Keller JJ, Keller AB, Picciotto MR, Paylor R, Booker TK, Beaudet A, Heinemann SF and Balogh SA (2004) Role of neuronal nicotinic receptors in the effects of nicotine and ethanol on contextual fear conditioning. *Neuroscience* 129:11-24.

Whiteaker P, Davies AR, Marks MJ, Blagbrough IS, Potter BV, Wolstenholme AJ, Collins AC and Wonnacott S (1999) An autoradiographic study of the distribution of binding sites for the novel alpha7-selective nicotinic radioligand [3H]-methyllycaconitine in the mouse brain. *Eur J Neurosci* 11:2689-2696.

Wishka DG, Walker DP, Yates KM, Reitz SC, Jia S, Myers JK, Olson KL, Jacobsen EJ, Wolfe ML, Groppi VE, Hanchar AJ, Thornburgh BA, Cortes-Burgos LA, Wong EH, Staton BA, Raub TJ, Higdon NR, Wall TM, Hurst RS, Walters RR, Hoffmann WE, Hajos M, Franklin S, Carey G, Gold LH, Cook KK, Sands SB, Zhao SX, Soglia JR, Kalgutkar AS, Arneric SP and Rogers BN (2006) Discovery of N-[(3R)-1-azabicyclo[2.2.2]oct-3-yl]furo[2,3-c]pyridine-5-

carboxamide, an agonist of the alpha7 nicotinic acetylcholine receptor, for the potential treatment of cognitive deficits in schizophrenia: synthesis and structure-activity relationship. *J Med Chem* 49:4425-4436.

Footnotes

This work was supported by Abbott Laboratories. The autoradiography work was supported, in part, by the Swiss National Science Foundation to DB.

Reprint requests:
David J. Anderson
R-47W, AP9A
Abbott Laboratories
Abbott Park, IL 60064-6125
Phone: 847-937-5830
FAX: 847-937-9195
Email: david.j.anderson@abbott.com

JPET Fast Forward. Published on October 24, 2007 as DOI: 10.1124/jpet.107.130062
This article has not been copyedited and formatted. The final version may differ from this version.

Legends for Figures

Fig. 1. Structures of [^{3}H]A-585539 and [^{3}H]MLA.

Fig. 2. Saturation binding isotherms of [^{3}H]A-585539. Binding of [^{3}H]A-585539 to membrane enriched fractions from rat brain (A) and human frontal cortex (B). Membranes were incubated for 90 min at 4°C with a range of 0.01 to 2 nM [^{3}H]A-585539. Shown are specific binding (quadruplicates) and non-specific binding (duplicates) which was measured in the presence of 10 μM MLA. Figures shown are one of eight independent experiments for each tissue. Data from saturation binding experiments were analysed by nonlinear regression, and the K_d and B_{max} values are shown in Table 1.

Fig. 3. Kinetics of [^{3}H]A-585539 binding to rat brain membranes. A, Dissociation of [^{3}H]A-585539. Samples in quadruplicate were equilibrated with 0.1 nM [^{3}H]A-585539 for 90 min at 4°C (closed symbols, solid line) or at 22°C (open symbols, dotted line). Then, the radioligand was displaced with 10 μM unlabelled A585539. Dissociation was terminated at various time intervals, as indicated, by rapid filtration onto 96-well glass fibre filter plates. Depicted is one experiment at each temperature for which the half-times ($t_{1/2}$) of dissociation for [^{3}H]A-585539 binding were 70.1 min at 4°C and 5.7 min at 22°C. The average $t_{1/2}$ values for dissociation were 64.2 ± 6.1 min at 4°C (n = 5) and 7.3 ± 0.5 min at 22°C (n = 4). B, Association of [^{3}H]A-585539. Samples in quadruplicate were incubated with 0.1 nM [^{3}H]A-585539 at 4°C (closed symbols, solid line) or at 22°C (open symbols, dotted line) for various time intervals as indicated. Association was terminated with rapid filtration onto 96-well glass fibre filter plates. Depicted is one experiment at each

JPET Fast Forward. Published on October 24, 2007 as DOI: 10.1124/jpet.107.130062
This article has not been copyedited and formatted. The final version may differ from this version.

temperature for which the half-times ($t_{1/2}$) of association for [^{3}H]A-585539 binding were 9.3 min at 4°C and 9.0 min at 22°C. The average $t_{1/2}$ values for association were 8.0 ± 0.8 min at 4°C (n = 5) and 7.4 ± 0.7 min at 22°C (n = 4).

Fig. 4. Displacement of [^{3}H]A-585539 binding. Concentration-inhibition curves for the displacement of [^{3}H]A-585539 binding to rat brain (A) and human cortex (B) membranes by three α7 nAChR compounds, MLA, PNU 282987 and racemic AR-R17779. Data points are the mean data from three independent experiments. The K_i values are summarized in Table 2. C, correlation plot for log K_i values of displacement of [^{3}H]A-585539 binding from rat brain versus human frontal cortex. Excluding MLA, there was good correlation with a slope of 0.94 and a coefficient of correlation of 0.88. Data points are the mean of 3-10 independent determinations from Table 2.

Fig. 5. Comparison of displacement of [^{3}H]A-585539 and [^{3}H]MLA binding from rat brain membranes by nAChR agonists and antagonists. Data points are the log K_i values from 3 to 11 independent determinations of data taken from Table 3. The coefficient of correlation and slope values are 0.96 and 0.95 respectively.

Fig. 6. Binding of [^{3}H]A-585539 to α7/5HT$_3$ chimera expressed in HEK-293 cells. A, Saturation binding of [^{3}H]A-585539 to α7/5HT$_3$ cell membranes. Represented is one of four independent experiments. Specific binding was determined in the presence of [^{3}H]A-585539 (0.05-10 nM; 90 min incubation at 4°C). Nonspecific binding was determined in the presence of 30 μM MLA. Data were analysed by nonlinear regression and the K_d and B_{max} values were determined for each experiment. The mean ± S.E.M. estimates for K_d was 0.80 ± 0.12 nM and for B_{max} was 10,500 ±

1000 fmol/mg protein. B, Comparison of displacement of [^{3}H]A-585539 binding from rat brain membranes and α7/5HT$_3$ chimera expressing cell membranes by nAChR ligands. Data points are log Ki values of 3-10 independent determinations for rat brain and 3-4 determinations for α7/5HT$_3$ cell membranes. The coefficient of correlation and slope values are 0.94 and 1.02 respectively

Fig. 7. Comparison of labeling obtained with [^{3}H]A-585539 and [^{125}I]α-bungarotoxin in the rat brain. Panels A-C are from 3 adjacent coronal sections cut through the diencephalon. Section A was incubated with 25 nM of [^{3}H]A-585539**;** sections B and C with 25 nM of [^{3}H]A-585539 together with 1 mM of nicotine tartrate (B) or 500 μM of unlabeled A-585539 (C). D and E are from two adjacent sections cut from another rat brain and incubated with 1 nM [^{125}I]-α-bungarotoxin either alone (D) or together with 300 μM of nicotine tartrate (E). Note that [^{3}H]A-585539 and [^{125}I]α-bungarotoxin yielded a similar labelling of field CA3 of the hippocampus (CA3) and of the superficial gray layer of the superior colliculus (SuG). Note also that [^{3}H]A-585539 binding in CA3 (A and B) is only partially displaced by nicotine tartrate (B) whereas it is not detectable in the presence of unlabeled A-585539 in excess (D). Bar = 5 mm.

JPET Fast Forward. Published on October 24, 2007 as DOI: 10.1124/jpet.107.130062
This article has not been copyedited and formatted. The final version may differ from this version.

Table 1. K_d and B_{max} values from [^{3}H]A-585539 Saturation Binding Analysis

Tissue	Temperature	K_d	B_{max}	n
		nM	fmol/mg protein	
Rat brain	4^{o}C	0.063 ± 0.004	33.7 ± 1.1	8
	22^{o}C	0.188 ± 0.013	31.7 ± 1.5	5
	37^{o}C	0.945 ± 0.103	42.1 ± 2.2	2
Human cortex	4^{o}C	0.066 ± 0.006	5.8 ± 0.5	8
α7/5HT$_3$ chimera	4^{o}C	0.80 ± 0.12	10,500 ± 1000	4

JPET Fast Forward. Published on October 24, 2007 as DOI: 10.1124/jpet.107.130062
This article has not been copyedited and formatted. The final version may differ from this version.

Table 2. Displacement of [^{3}H]A-585539 binding to rat and human brain: Comparison with [^{3}H]MLA

Ligand	[^{3}H]A-585539								[^{3}H]MLA			
	Rat				Human				Rat			
Compound	Ki, nM	95% c.i.	nH	n	Ki, nM	95% c.i.	nH	n	Ki, nM	95% c.i.	nH	n
A-585539	0.071	0.06-0.09	0.8	4	n.d.				1.01	0.6-1.6	1.0	4
MLA	0.19	0.16-0.23	1.1	10	2.5	1.8-3.6	0.9	9	2	1.5-2.7	1.1	10
TC-5280	0.36	0.33-0.38	0.9	3	n.d.				1.2	0.9-1.5	1.6	3
Epibatidine	2.7	2.1-3.4	1.0	8	1.1	0.7-1.7	0.8	3	21	13-33	1.4	4
PNU 282987	6.5	5.8-7.2	0.9	7	3.2	2.2-4.5	0.9	6	46.4	33-66	1.1	6
A-582941	10.8	6.2-19	1.1	9	16.7	13-22	1.1	6	88	59-130	1.7	11
α-Bungarotoxin	12.2	9.4-16	2.1	3	17.7	8.1-39	0.9	2	17.4	14-21	1.2	3
Anatoxin-A	19.8	16-24	1.2	5	9.7	7.1-13	1.1	4	122	97-150	1.6	6
Varenicline	33.4	23-49	1.2	6	15.6	12.0-20	0.9	6	144	100-210	1.3	7
A-85380	33.6	20-57	1.1	4	17.6	6.4-48	0.9	2	299	150-610	1.6	4
(±)-AR-R17779	128	100-160	1.0	5	40.5	27-60	1.0	6	1390	1100-1760	1.5	5
(-)-Nicotine	176	62-500	1.1	8	159	110-230	1.0	6	1450	850-2500	1.6	6
DMPP	308	220-420	1.5	4	153	110-210	1.7	3	1580	1200-2100	1.6	4

c.i., 95% confidence interval; n = number of determinations, each carried out in duplicate.

JPET #130062

Figure 1

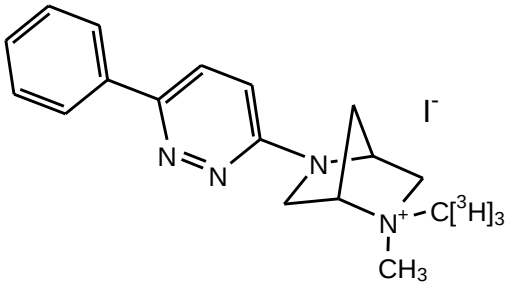

[^{3}H]A-585539

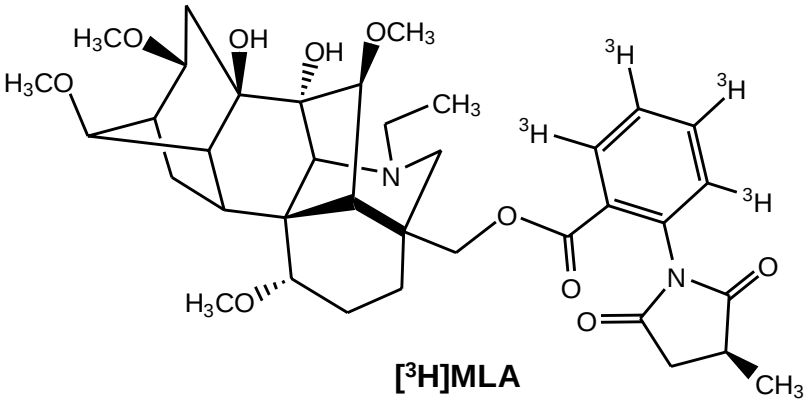

[^{3}H]MLA

Figure 2

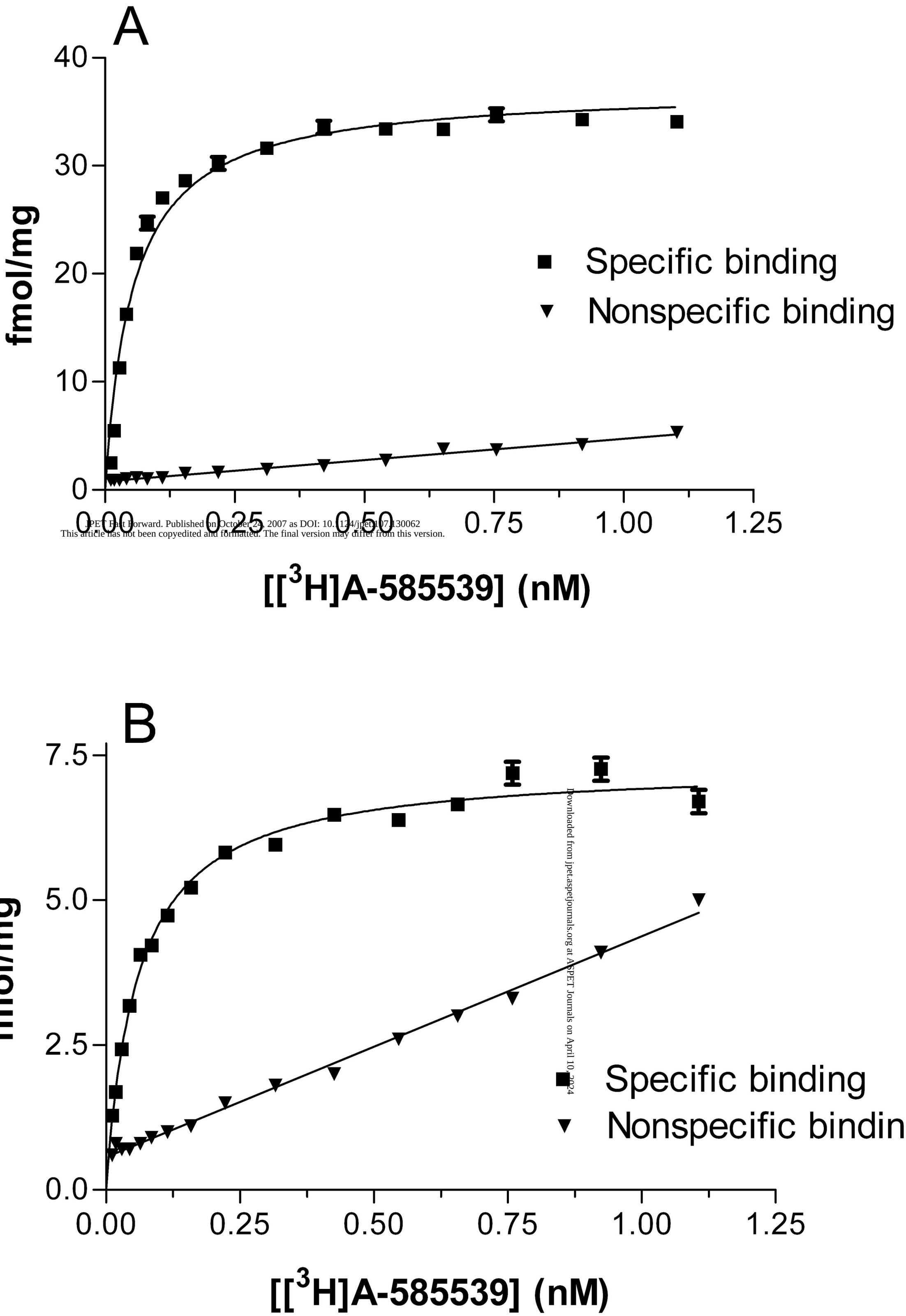

Figure 3

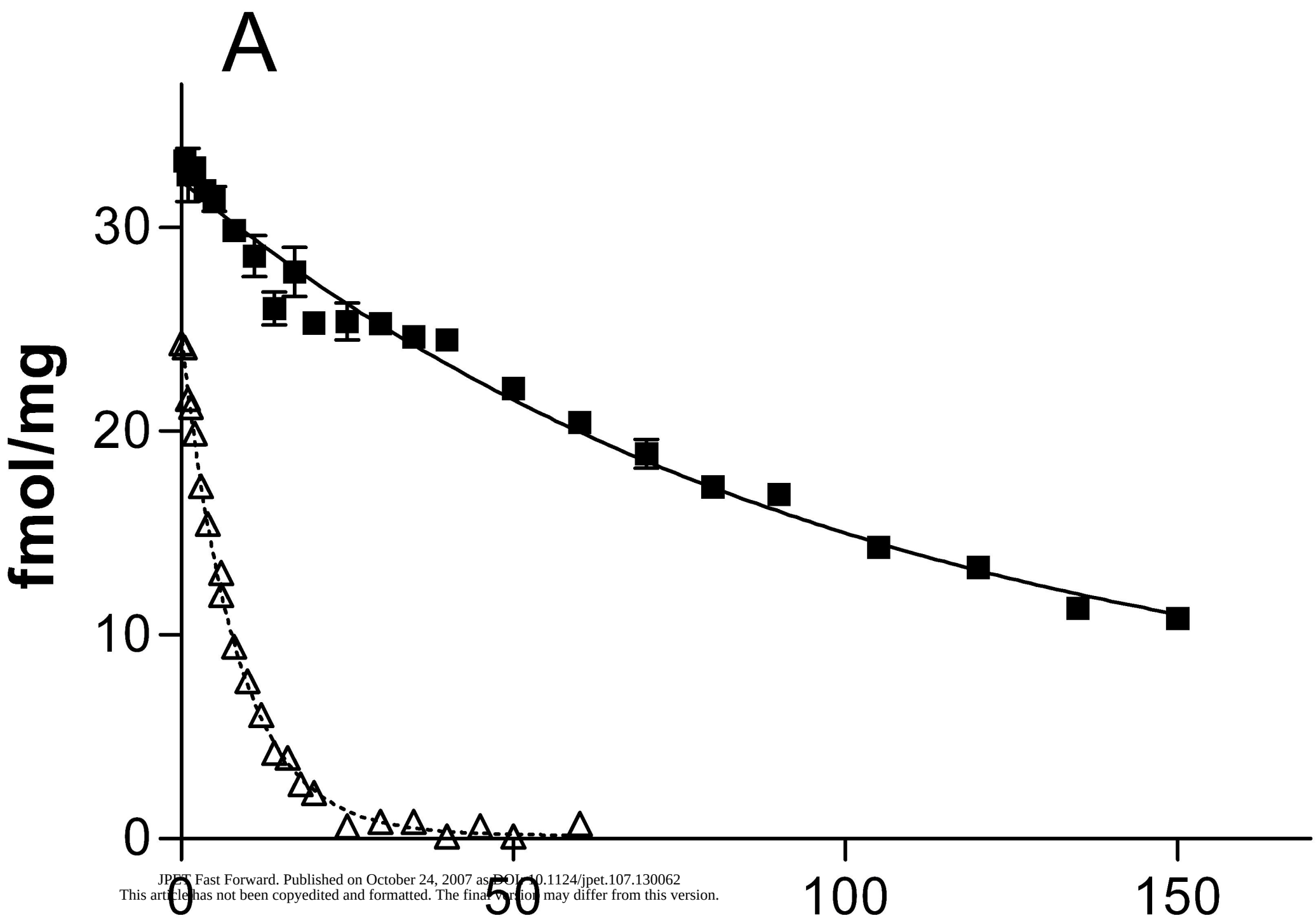

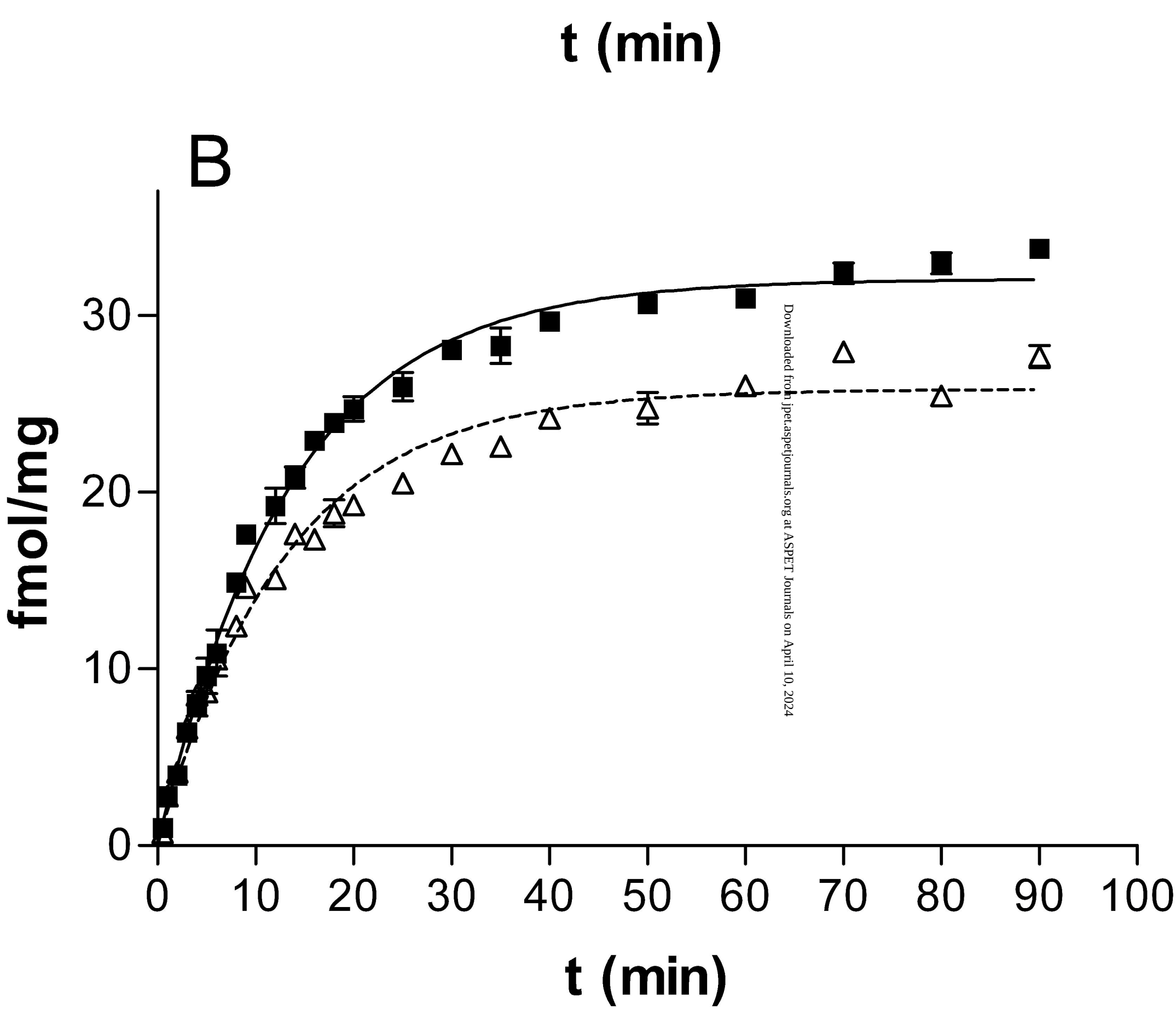

Figure 4

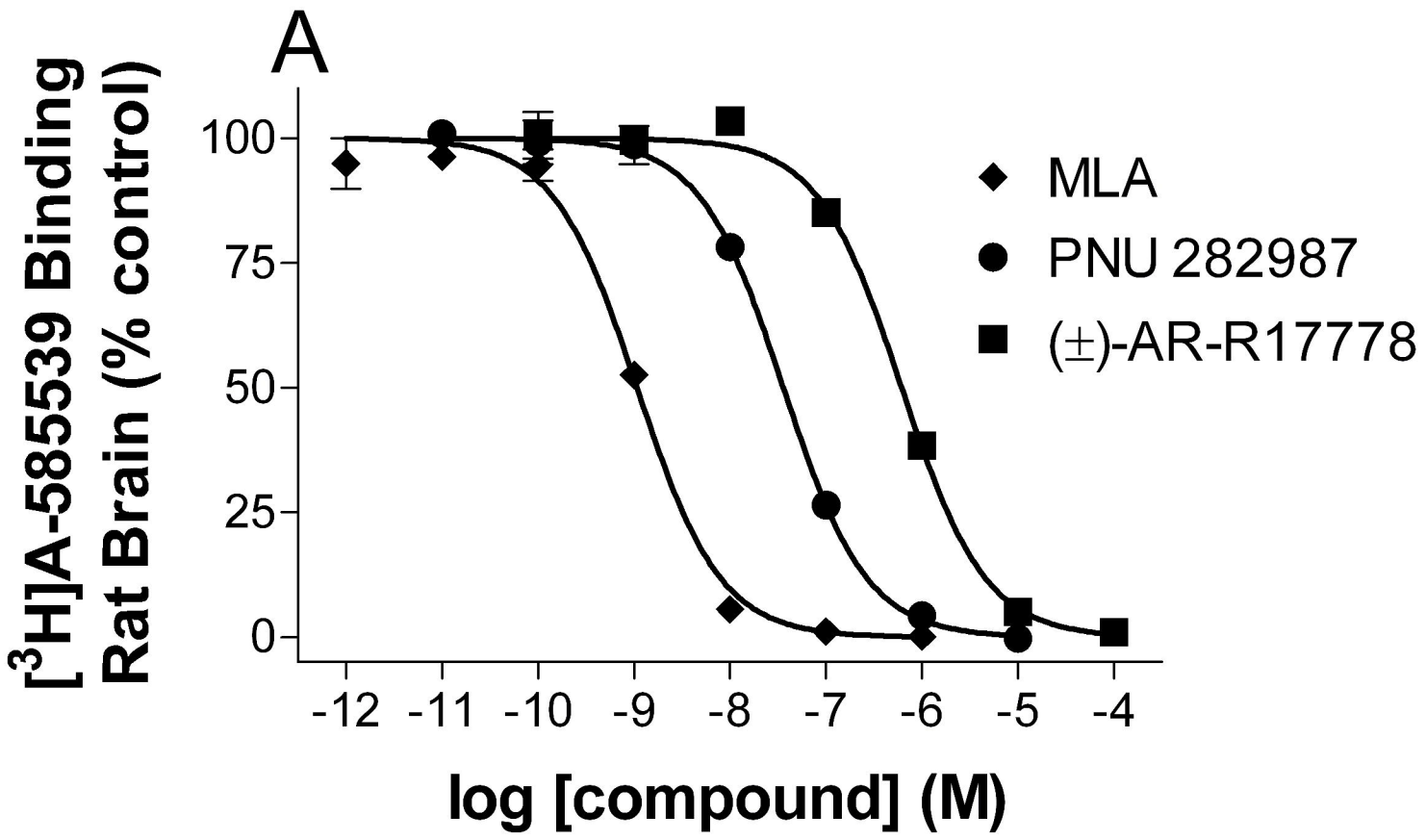

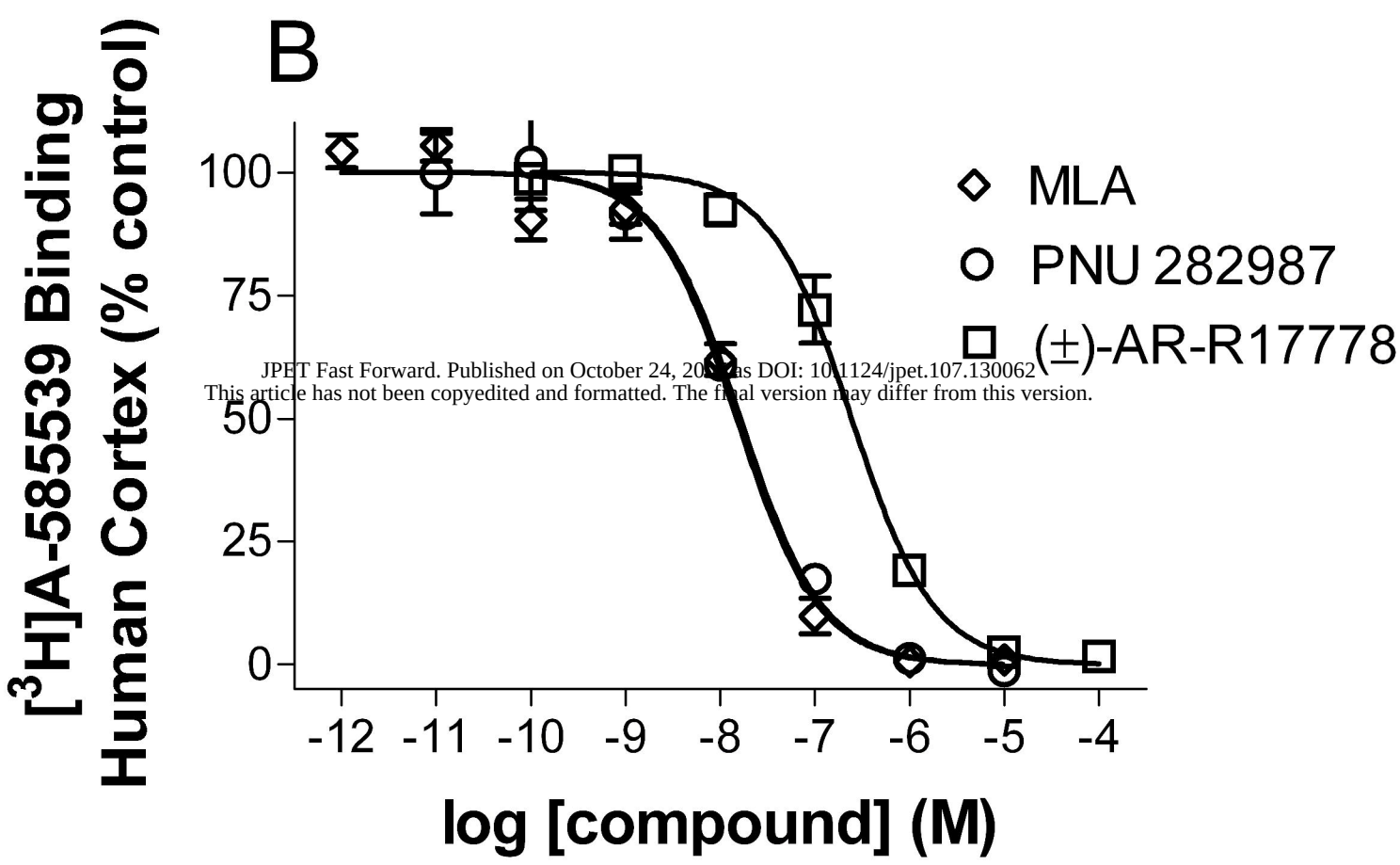

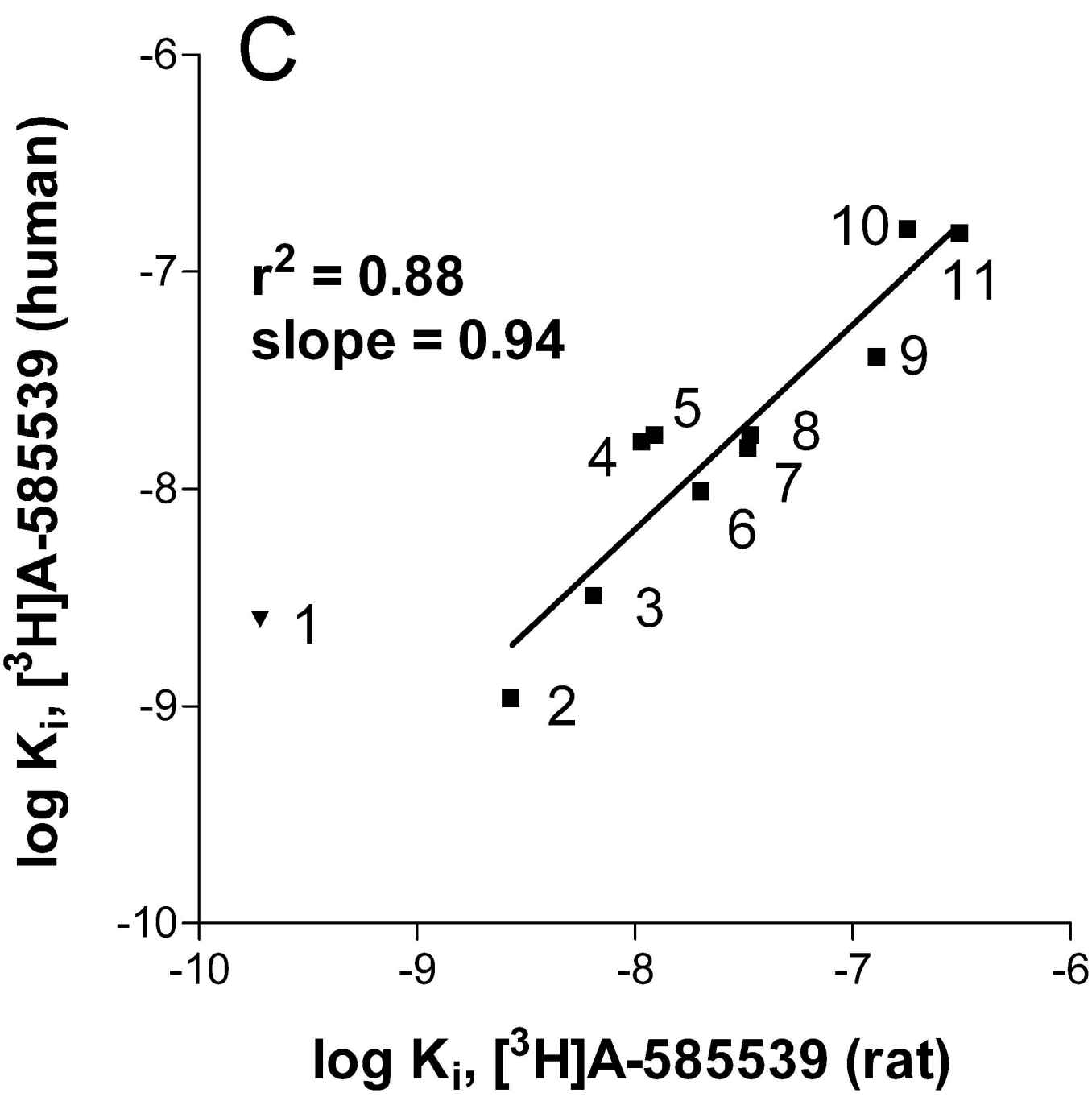

1. MLA
2. Epibatidine
3. PNU 282987
4. A-582941
5. α-Bungarotoxin
6. Anatoxin-A
7. Varenicline
8. A-85380
9. (±)-AR-R17779
10. (-)-Nicotine
11. DMPP

Figure 5

JPET Fast Forward. Published on October 24, 2007 as DOI: 10.1124/jpet.107.130062
This article has not been copyedited and formatted. The final version may differ from this version.

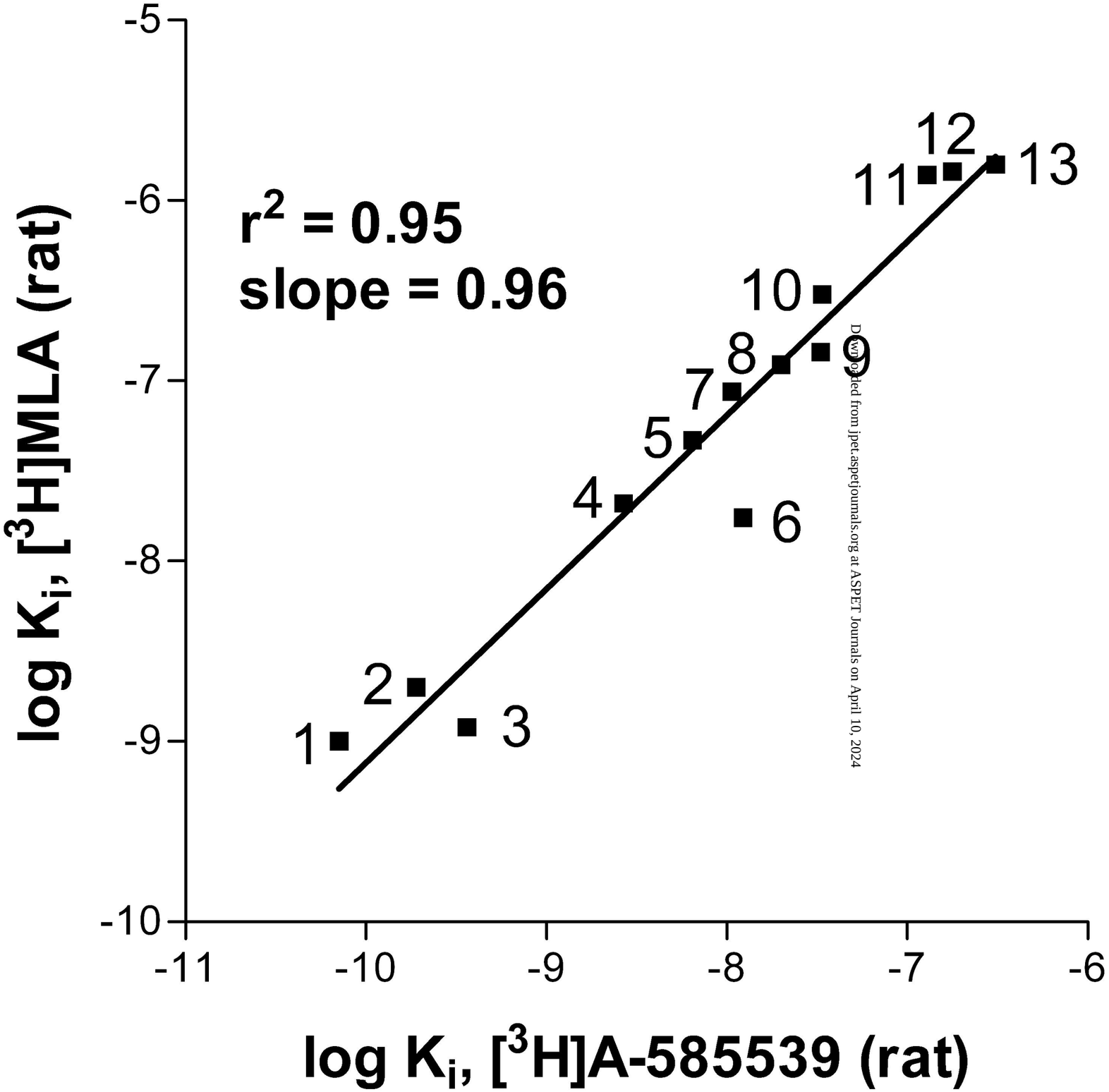

1. A-585539
2. MLA
3. TC-5280
4. Epibatidine
5. PNU 282987
6. α-Bungarotoxin
7. A-582941
8. Anatoxin-A
9. Varenicline
10. A-85380
11. ($\pm$)-AR-R17779
12. (-)-Nicotine
13. DMPP

Figure 6

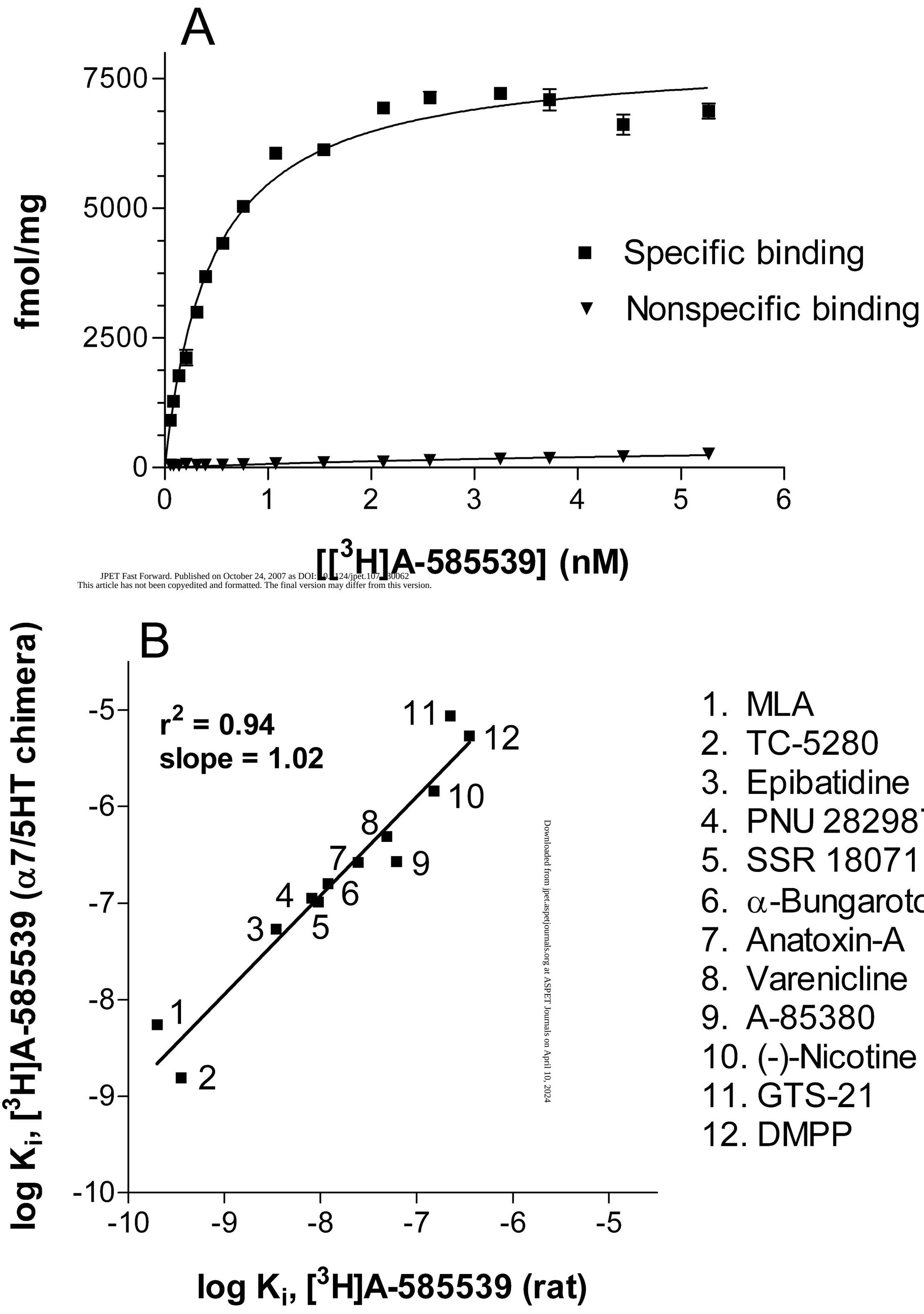

JPET Fast Forward. Published on October 24, 2007 as DOI: 10.1124/jpet.107.130062
This article has not been copyedited and formatted. The final version may differ from this version.

JPET Fast Forward. Published on October 24, 2007 as DOI: 10.1124/jpet.107.130062
This article has not been copyedited and formatted. The final version may differ from this version.

JPET #130062

Figure 7